Tunable Feshbach Resonances and Their Spectral Signatures in Bilayer Semiconductors

Author(s):
Kuhlenkamp, Clemens; Knap, Michael; Wagner, Marcel; Schmidt, Richard; Imamoglu, Atac

Publication date:
2022-07-15

Permanent link:
https://doi.org/10.3929/ethz-b-000558331

Originally published in:
Physical Review Letters 129(3), https://doi.org/10.1103/physrevlett.129.037401

Tunable Feshbach Resonances and Their Spectral Signatures in Bilayer Semiconductors

Clemens Kuhlenkamp,[1,2,3] Michael Knap,[2,3] Marcel Wagner,[4,3] Richard Schmidt,[4,3] and Ataç Imamoğlu[1]
[1]Institute for Quantum Electronics, ETH Zürich, CH-8093 Zürich, Switzerland
[2]Department of Physics and Institute for Advanced Study, Technical University of Munich, 85748 Garching, Germany
[3]Munich Center for Quantum Science and Technology (MCQST), Schellingstraße 4, D-80799 München, Germany
[4]Max-Planck-Institute of Quantum Optics, Hans-Kopfermann-Straße 1, 85748 Garching, Germany

(Received 10 May 2021; revised 7 November 2021; accepted 27 June 2022; published 12 July 2022)

Feshbach resonances provide an invaluable tool in atomic physics, enabling precise control of interactions and the preparation of complex quantum phases of matter. Here, we theoretically analyze a solid-state analog of a Feshbach resonance in two dimensional semiconductor heterostructures. In the presence of interlayer electron tunneling, the scattering of excitons and electrons occupying different layers can be resonantly enhanced by tuning an applied electric field. The emergence of an interlayer Feshbach molecule modifies the optical excitation spectrum, and can be understood in terms of Fermi polaron formation. We discuss potential implications for the realization of correlated Bose-Fermi mixtures in bilayer semiconductors.

DOI: 10.1103/PhysRevLett.129.037401

Recently, bilayer structures of two-dimensional materials have emerged as fascinating platforms for realizing exotic phases of electronic matter [1,2]. Much of their success is driven by a new level of control, arising from twisting the two layers with respect to each other during stacking. Such twisted bilayers generate a moiré potential for electrons or holes, which quenches the kinetic energy and therefore enhances correlations. Most notably this has lead to the discovery of unconventional superconductivity [3,4], correlated insulators, and generalized Wigner crystals [5–7] in bilayer graphene and transition metal dichalcogenides (TMDs). In addition to electronic phases, semiconductors such as TMDs can host excitons, which are strongly bound electron-hole pairs. They act as mobile composite bosons and remain rigid due to their large binding energies. Moreover, excitons interact with free electrons or holes and can form charged molecules, termed trions. This renders bilayer TMDs promising candidates to study complex Bose-Fermi mixtures. Such mixtures have been recently investigated in dilute quantum gases [8–10], where Feshbach resonances are routinely used to control interactions between the atomic species [11–15]. By contrast, in solid state structures the molecular binding energies, and correspondingly the interaction strength among particles, are generically fixed by material properties, limiting the experimentally accessible regimes.

Here, we address this challenge by introducing a solid-state analog of a Feshbach resonance. Using the layer degree of freedom as a pseudospin, we demonstrate that the energy of a closed-channel bound state can be tuned with respect to scattering states in an open channel, simply by applying an external electric field E_z. The counterpart of hyperfine interactions in atomic systems, is provided by coherent interlayer electron or hole tunneling. The emerging Feshbach molecule controls the interlayer scattering and originates from the hybridization of exciton-electron scattering states with the intralayer (closed channel) trion state [16]. As such, it is fundamentally distinct from the formation of interlayer trions due to interactions determined by the material properties that are not tunable [17]. We demonstrate the impact of such Feshbach resonances on the spectrum of a single optically injected exciton immersed in a Fermi sea of charge carriers, taking into account the radiative exciton decay. Close to the Feshbach resonance we find a striking modification of the exciton spectrum. In particular, we show that the spectral shape is sensitive to the finite range of the effective interactions relative to the Fermi wavelength.

Our Letter is motivated by a recent experimental observation of an electrically tunable Feshbach resonance in a twisted bilayer TMD heterostructure [18]. We theoretically analyze a more generic scenario with vanishing twist angles and discuss how resonantly enhanced polaron formation can be observed in reflection measurements. Our findings demonstrate the potential for bilayer TMDs to control valley-selective interactions between itinerant carriers and establish a novel platform for exploring correlated quantum dynamics of degenerate Bose-Fermi mixtures.

Effective bilayer Hamiltonian.—We consider a bilayer semiconductor setup as depicted in Fig. 1. As we are

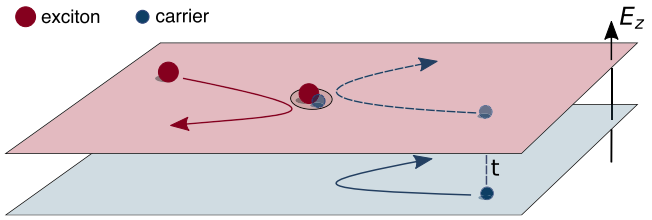

FIG. 1. Tunable Feshbach resonances in bilayer heterostructures. Illustration of exciton-carrier scattering in a bilayer TMD. The electrostatic potential energy is different in the two layers and can be tuned by a perpendicular electric field E_z. Scattering between excitons and electrons is enhanced when the intralayer trion energy is tuned into resonance with the energy of an electron and an exciton in separate layers.

interested in low-energy scattering, details of the underlying atomic lattice are irrelevant due to the large separation of scales between the lattice momentum and the momenta of excitons and electrons. In this regime excitons and electrons have essentially parabolic dispersions. Tunneling of electrons (or holes) between the two layers can be described by an effective average coupling constant t, which can be adjusted by incorporating tunnel barriers [7,19]. For concreteness we focus on two identical TMD layers separated by a distance d. Generically, the exciton resonances in the top and bottom layers have different energies, either due to the difference in material properties or strain, enabling layer-selective exciton creation. Furthermore, for electric fields close to the Feshbach resonance, the hybridization of inter- and intralayer excitons is small due to their sizable energy difference. This allows us to focus only on intralayer excitons [20]. For simplicity we assume that excitons are injected optically and are present only in the top layer. The system is then described by the effective Hamiltonian

$$\hat{H} = \sum_{\mathbf{k}} x^\dagger_{\mathbf{k}} \frac{k^2}{2M} x_{\mathbf{k}} + \begin{pmatrix} c^\dagger_{\mathbf{k},T} \\ c^\dagger_{\mathbf{k},B} \end{pmatrix} \begin{pmatrix} \xi_{\mathbf{k}} + \Delta & t \\ t & \xi_{\mathbf{k}} \end{pmatrix} \begin{pmatrix} c_{\mathbf{k},T} \\ c_{\mathbf{k},B} \end{pmatrix} + \frac{U}{V} \sum_{kk'q} c^\dagger_{\mathbf{k},T} c_{\mathbf{k}+\mathbf{q},T} x^\dagger_{\mathbf{k}'} x_{\mathbf{k}'-\mathbf{q}}, \tag{1}$$

where $x^\dagger_{\mathbf{k}}$ creates an exciton of mass M in the top layer, and $c^\dagger_{\mathbf{k},T}$ and $c^\dagger_{\mathbf{k},B}$ create fermions of mass m in the top and bottom layer, respectively.

From now on we refer to itinerant charges as electrons, although all conclusions apply equally to holes. We omit the valley and spin degree of freedom and assume that electrons and excitons reside in different valleys, since only this scattering channel will be resonantly enhanced. As the exciton's Bohr radius is small, excitons and electrons experience sizable attractive contact interactions U, only when both particles are in the same layer and opposite valleys. We also neglect the composite nature of the exciton and treat it as a structureless boson [21]. The potential energy difference $\Delta = qdE_z$ between the two layers, can be tuned by changing E_z, as illustrated in Fig. 1. We consider the scenario where Δ is chosen such that electrons reside predominantly in the bottom layer.

Feshbach resonance in exciton-electron scattering.—To understand scattering properties in such a heterostructure, we focus on the two-particle subspace of the system. In the center of mass frame, Eq. (1) can then be expressed in first quantization as

$$\begin{aligned} \hat{H}_{2\,\mathrm{body}} &= \hat{H}_0 + \hat{U} \\ &= \begin{pmatrix} -\frac{\nabla^2_{\mathbf{R}}}{2m_{\mathrm{tot}}} - \frac{\nabla^2_{\mathbf{r}}}{2\mu} + \Delta & t \\ t & -\frac{\nabla^2_{\mathbf{R}}}{2m_{\mathrm{tot}}} - \frac{\nabla^2_{\mathbf{r}}}{2\mu} \end{pmatrix} \\ &\quad + U \begin{pmatrix} \delta^2(\mathbf{r}) & 0 \\ 0 & 0 \end{pmatrix}, \end{aligned} \tag{2}$$

where $\mu = 1/(m^{-1} + M^{-1})$ and $m_{\mathrm{tot}} = m + M$ are the reduced mass and the total mass, respectively. The wave function carries the layer degree of freedom and the part describing the relative motion can be expressed as $\psi(\mathbf{r}) = [\psi_T(\mathbf{r}), \psi_B(\mathbf{r})]^T/\sqrt{2}$. Asymptotic eigenstates with large spatial separation between the two particles define the open and closed channel. We consider E_z for which $\Delta \simeq |E^0_B|$, where E^0_B is the binding energy of the intralayer trion. Although both channels are hybridized between the layers, only the open channel is energetically accessible and electrons reside predominantly in the bottom layer (Fig. 2). The scattering threshold for the open (ε_O) and closed (ε_C) channel is $\varepsilon_{O,C} = \Delta/2 \mp \sqrt{t^2 + \Delta^2/4}$.

The outgoing scattering states $|\psi^+_\alpha\rangle$, in channel α with energy E can be found as solutions of the Lippmann-Schwinger equation:

$$|\psi^+_\alpha\rangle = |\phi_\alpha\rangle + \frac{1}{E - \hat{H}_0 + i0^+} \hat{U} |\psi^+_\alpha\rangle, \tag{3}$$

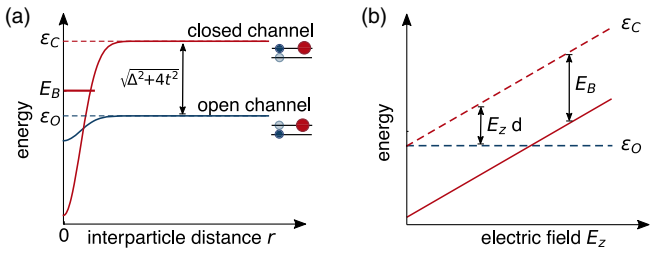

FIG. 2. Illustration of scattering channels. (a) Interparticle potential for an exciton and an electron prepared in the open (blue) or closed (red) channel. Tunnel coupling imprints the closed channel attraction also on the open channel. (b) Threshold energies of the open and closed channel ε_O and ε_C, as the electric field is varied. The bare closed channel bound-state energy is denoted as a red line. This bound state can be brought into resonance with ε_O for an appropriately chosen electric field.

where $\langle \mathbf{r}|\phi_\alpha\rangle \sim e^{ikx}$ is an incoming plane wave [15,22,23]. We can reformulate the problem by introducing the T matrix $\hat{T}^R|\phi_\alpha\rangle = \hat{U}|\psi_\alpha^+\rangle$, which connects the incoming plane waves with the full outgoing scattering state. Equation (3) translates to an equation for the off-shell T matrix $\hat{T}^R(E)$:

$$\hat{T}^R(E) = \hat{U} + \hat{U}(E - \hat{H}_0 + i0^+)^{-1}\hat{T}^R(E). \tag{4}$$

We solve Eq. (4) analytically in a plane-wave basis which diagonalizes $\hat{H}_0$:

$$\hat{T}^R(E,\mathbf{k}) = [\mathbb{1}_{2\times 2} - \hat{U}\cdot\Pi^R(E,\mathbf{k})]^{-1}\cdot\hat{U},$$
$$\Pi^R_{\alpha\beta}(E,\mathbf{k}) = \int \frac{d^2q}{(2\pi)^2}\frac{\delta_{\alpha\beta}}{E - \frac{\mathbf{q}^2}{2\mu} - \frac{\mathbf{k}^2}{2m_{\mathrm{tot}}} - \varepsilon_\alpha + i0^+}, \tag{5}$$

where E is the scattering energy, and $\mathbf{k}$ is the total incoming momentum. The 2×2 matrix structure of $\hat{T}^R(E,\mathbf{k})$, and $\hat{U}$, due to the two channels, is implicitly assumed.

Scattering can be resonantly enhanced if E_z is tuned such that the closed channel bound state is in proximity of the open channel threshold ε_O, see Fig. 2(b) for an illustration. Similar to cold atomic systems, we are interested in two-particle collisions with small incoming momenta. In this case, scattering is accurately described by a finite-range expansion, which is performed by expanding the denominator of the T matrix in powers of $E - \varepsilon_O$. In two dimensions the finite range expansion of the on-shell T matrix takes the universal form

$$T^R(\mathbf{q}^2/2\mu,\mathbf{0})^{-1} = \frac{\mu}{2\pi}\left(i\pi - \ln(\mathbf{q}^2a^2) + \frac{r_0\mathbf{q}^2}{2} + \mathcal{O}(\mathbf{q}^3)\right), \tag{6}$$

which is characterized by the scattering length a and effective range r_0 [24,25]. We relate this expansion to our effective description by integrating Eq. (5) and matching the open channel scattering amplitude $T^R_{OO}(\mathbf{q}^2/2\mu,\mathbf{0})$ to Eq. (6). In this way we obtain the open channel scattering length a_O and effective range r_0:

$$a_O = a\exp\left\{-\frac{1}{2}\left(\frac{\Delta}{2t} + \sqrt{1+\frac{\Delta^2}{4t^2}}\right)^2 \ln\frac{-E_B^0}{\sqrt{4t^2+\Delta^2}}\right\},$$
$$r_0 = \frac{1}{2\mu}\frac{(\Delta/2 + \sqrt{t^2+\Delta^2/4})^2}{t^2\sqrt{t^2+\Delta^2/4}}, \tag{7}$$

where $a = 1/\sqrt{2\mu E_B^0}$ is the scattering length of the closed channel in the absence of tunnel coupling. Analyzing Eqs. (5)–(7), we find that the open channel T matrix has a pole at energies below the scattering threshold ε_O. This is the signature of a Feshbach molecule which forms in interlayer scattering [23]. Equation (6) demonstrates that the energy of the molecule depends on both the scattering length a_O and range r_0. We plot the energy of the Feshbach molecule as a function of detuning in Fig. 3 for three different t. As the detuning becomes large and positive, the scattering length starts to diverge while the molecular energy approaches the scattering threshold. For large detunings the binding energy is then approximately given by $1/2\mu a_O^2$.In the case $\Delta > E_B^0 \gg t$ we obtain simple expressions for the binding energy of the Feshbach molecule E_B and the effective range close to resonance, which reads

$$E_B \simeq E_B^0\frac{1}{e^{-2}}\left|\frac{\Delta}{E_B^0}\right|^{-\Delta^2/t^2}, \qquad r_0 \simeq \frac{1}{\mu}\frac{\Delta}{t^2}. \tag{8}$$

This demonstrates the power of a Feshbach resonance: complete control over the energy of the Feshbach molecule can be achieved simply by changing E_z. Thus the system can be electrically tuned to arbitrarily large scattering lengths [26,27]. While the binding energy of the Feshbach molecule changes exponentially, the effective range r_0 depends only linearly on E_z. We find that weakly coupled layers lead to large values of r_0, and the resulting physics is reminiscent of narrow Feshbach resonances in three dimensions.

In contrast to the three dimensional case, however, the bound state does not dissolve for any value of E_z, as long as

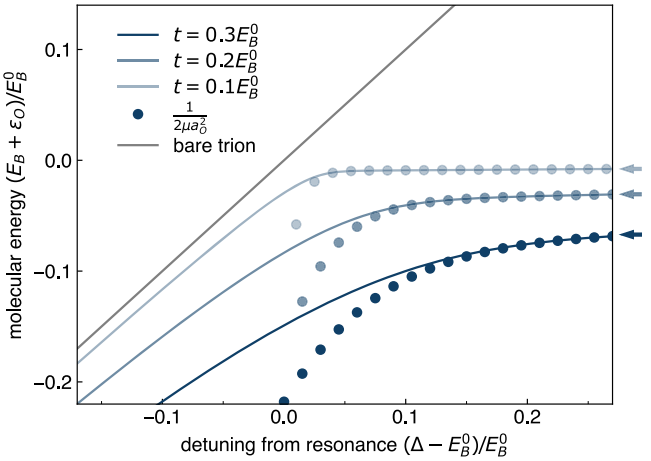

FIG. 3. Feshbach molecule binding energy. Molecular energy as a function of electric field (solid blue lines). We have assumed an exciton mass of $M = 2m$ and contact interactions between the exciton and electron. In two dimensions, and in the absence of interlayer repulsion, a bound state exists for all values of Δ. When the size of the molecule exceeds the range of the interactions, the scattering length alone determines the binding energy (blue dots). For large positive detunings the molecular energy approaches the open channel threshold ε_O (arrows), implying that the binding energy E_B goes asymptotically to zero. For large negative detunings the binding energy approaches the energy of the bare intralayer trion.

there is no repulsive background scattering [28]. The purely two dimensional geometry of the system also distinguishes the proposed resonance from realizations in cold atom systems, where scattering remains effectively three dimensional due to the finite transverse confinement [14].

Optical impurities strongly coupled to a Fermi sea.—Resonantly enhanced two-particle scattering affects correlations in electron-exciton mixtures. We consider a low concentration of excitons injected into a Fermi sea of electrons in the open channel. The excitons in such a system are mobile impurities and form collective excitations known as Fermi polarons [30–34]. Here, we analyze the polaron spectrum as E_z is tuned over the Feshbach resonance.

Our previous discussions focused on two-body scattering with small but finite momentum, for which the exciton is long-lived and the scattering matrix is essentially unitary [35]. Here, we focus on optically excited $\mathbf{k} = 0$ excitons. In this regime excitons couple to the radiation field, which allows them to decay via electron-hole recombination via the emission of an optical photon. As this decay process is essentially memoryless, it can be described by a Lindblad master equation

$$\dot{\rho}(t) = -i[\hat{H}, \rho] + \sum_{\mathbf{k}} L_{\mathbf{k}} \rho L_{\mathbf{k}}^{\dagger} - \frac{1}{2}\{L_{\mathbf{k}}^{\dagger} L_{\mathbf{k}}, \rho\},$$
$$L_{\mathbf{k}} = \sqrt{2\Gamma(\mathbf{k})}\, x_{\mathbf{k}}, \tag{9}$$

where $\Gamma(\mathbf{k})$ is the decay rate of the exciton, which we approximate to be finite only for $\mathbf{k} = 0$, due to the steep light cone of the photons. In the presence of a Fermi sea Eq. (9) constitutes a complex many-body system, which can not be solved exactly. However, it was found that key properties can already be inferred purely from the scattering properties of the system [36,37] and that T-matrix approximations provide an accurate description of the ground and excited states of mobile impurities [25,38–45].

For our heterostructure setting we develop a T-matrix approximation to include dissipation as well as finite-range corrections from the Feshbach resonance:

$$\hat{T}^R(E, \mathbf{k}) = [\mathbb{1}_{2\times 2} - \hat{U} \cdot \Pi^R(E, \mathbf{k})]^{-1} \cdot \hat{U}$$
$$\Pi^R_{\alpha\beta}(E, \mathbf{k}) = \int_{|\mathbf{q}'|>k_F} \frac{d^2q'}{(2\pi)^2} \frac{\delta_{\alpha\beta}}{E - \xi_{\mathbf{q}'} - \varepsilon_{\alpha} - \frac{(\mathbf{k}-\mathbf{q}')^2}{2M} + i\Gamma(\mathbf{k}-\mathbf{q}')}. \tag{10}$$

Details on the calculation can be found in the Supplemental Material [28]. Compared to Eq. (5), the momentum of the electron in the open channel is now restricted to lie above the Fermi surface due to Pauli blocking by the Fermi sea. Exciton recombination results in an imaginary part $i\Gamma(\mathbf{k})$ of the exciton energy [46,47]. Using this T matrix, we then determine the self-energy of the exciton as a function of frequency ω:

$$\Sigma^R(\omega, \mathbf{k}) = \int_{|\mathbf{q}|<k_F} \frac{d^2q}{(2\pi)^2} T^R_{OO}(\omega + \xi_{\mathbf{q}}, \mathbf{k} + \mathbf{q}). \tag{11}$$

This equation originates from the creation of a particle-hole pair in the open channel, with hole momentum $\mathbf{q} < k_F$. The spectral function of the exciton then reads

$$A_x(\omega, \mathbf{k}) = -2\mathrm{Im}\left[\frac{1}{\omega - \mathbf{k}^2/2M - \Sigma^R(\omega, \mathbf{k}) + i\Gamma(\mathbf{k})}\right]. \tag{12}$$

As the master equation fulfills fluctuation-dissipation relations and we have treated dissipation exactly, the resulting spectral function respects the sum rule $\int (d\omega/2\pi) A_x(\omega, \mathbf{k}) = \langle [x_{\mathbf{k}}, x_{\mathbf{k}}^{\dagger}] \rangle = 1$.

We compute the spectrum as a function of detuning, by integrating Eq. (12) numerically. We show the resulting

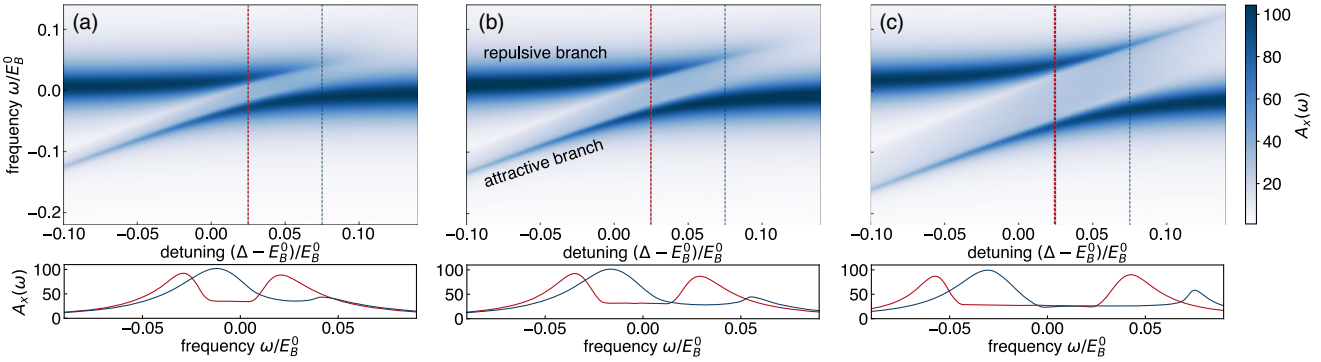

FIG. 4. Exciton spectra across the Feshbach resonance. The zero-momentum spectral function $A_x(\omega)$ of a dissipative exciton as a function of the bias Δ, computed within a T-matrix approximation. The Fermi energy E_F is increasing from left to right: (a) $E_F = E_B^0/30$, (b) $E_F = E_B^0/20$, (c) $E_F = E_B^0/10$. All spectra are computed for weak channel coupling $t = 0.15E_B^0$. The splitting of the repulsive and attractive branch depends on E_F, as highlighted in the line cuts of the spectra for two different Δ in the lower panels. For large E_F, finite range corrections become increasingly important and the repulsive branch is stabilized and regains oscillator strength. Motivated by recent experiments, the exciton is assumed to have a radiative lifetime of $\Gamma = E_B^0/30$ [49,50].

exciton spectra in Fig. 4 for three different Fermi energies (a)–(c). They are characterized by the formation of an attractive branch, with maxima at negative frequencies; and a repulsive branch, with maxima at positive frequencies. For small Fermi energies [Fig. 4(a)] the two resonances approach the Feshbach molecule and bare exciton energy, respectively: the spectrum can be understood in terms of the formation of a Fermi polaron and is highly asymmetric. We observe that the repulsive polaron abruptly transfers spectral weight to the attractive branch as the Feshbach molecule becomes weakly bound and blueshifts in energy.

With increasing carrier density, the maximal splitting between the repulsive and attractive branch grows [Fig. 4(b)]. Surprisingly, we find that the repulsive polaron branch is stabilized with growing electron densities, as seen in Fig. 4(c), despite the possible relaxation channel via excitations in the Fermi sea. This change in spectral shape cannot be explained assuming contact interactions, but rather arises from significant finite range corrections [48,51]. Since the average scattering process involves momenta on the order of k_F, the nonlogarithmic terms in Eq. (6) become successively more important at high densities and strongly renormalize the spectrum. In our setup Feshbach resonances are rather broad, which leads to characteristic spectral asymmetries due to the strong coupling to a continuum of scattering states. For Feshbach resonances based on polaritons on the other hand, this coupling is typically very weak due to the steep polariton dispersion, which can obscure the relevant scattering physics [52]. As the spectral function of the exciton is directly accessible in reflection measurements, the features we identified provide particularly clear experimental signatures, which result from many-body effects.

Conclusions and outlook.—We have investigated an electrically tunable solid-state Feshbach resonance, using the layer pseudospin degree of freedom of semiconductor bilayers. Our scheme allows for a controlled enhancement of electron-exciton scattering in experiments. We find that much of the resulting Feshbach physics, such as Fermi-Polaron formation for a dilute concentration of excitons, may be observed in experiments as a highly asymmetric and density-dependent reflection spectrum. This makes TMD bilayers ideal systems to study two dimensional Fermi polarons in parameter regimes that have so far been inaccessible in cold atomic gases and monolayer semiconductors.

By extending our setup to finite exciton densities, Feshbach resonances could enable precise control of degenerate Bose-Fermi mixtures in solid state systems. This is particularly appealing as excitations of an excitonic Bose gas can mediate superconductivity in a Fermi sea [53,54]. Since the bound state exists only for excitons and electrons with a different spin-valley degree of freedom, the Feshbach resonance could allow for spin selective interaction control and may induce instabilities in exotic pairing channels.

Feshbach resonances can also form in different scattering channels than the one considered here, i.e., an electron and an interlayer exciton in resonance with an intralayer bound state, which could prove to be useful in the context of long-lived indirect exciton condensates [55]. This is possible as interlayer and intralayer excitons have been shown to hybridize due to tunneling, and the energy of the former can be tuned electrically [7,56]. We further remark that while we discuss structures consisting of two identical TMD layers, the emerging Feshbach physics is universal. By choosing different TMDs and spacer materials one can vary the tunnel coupling and therefore the resonance width r_0.

Furthermore, our results generate the opportunity to study few-body physics in two dimensional semiconductors. The tunable scattering length can be used to explore exotic multiparticle bound states, where a single electron binds multiple excitons [57,58]. While we specifically considered resonant scattering between excitons and electrons, Feshbach physics in 2D materials could be a generic phenomenon that may also be relevant for understanding purely electronic processes [59].

We thank I. Schwartz and Y. Shimazaki for discussions which motivated this work. The authors also thank A. Cavalleri, F. Helmrich, and P. A. Murthy for fruitful discussions. This work was supported by ETH Zurich. We also acknowledge support from the Technical University of Munich–Institute for Advanced Study, funded by the German Excellence Initiative and the European Union FP7 under Grant No. 291763, the Deutsche Forschungsgemeinschaft (DFG, German Research Foundation) under Germany's Excellence Strategy–EXC–2111–390814868, TRR80 and DFG Grant No. KN1254/1-2, from the European Research Council (ERC) under the European Union's Horizon 2020 research and innovation programme (Grant No. 851161), as well as the priority program "Giant interactions in Rydberg systems," DFG SPP 1929 GiRyd, Grant No. 428462134.

[1] Eva Y. Andrei, Dmitri K. Efetov, Pablo Jarillo-Herrero, Allan H. MacDonald, Kin Fai Mak, T. Senthil, Emanuel Tutuc, Ali Yazdani, and Andrea F. Young, The marvels of moiré materials, Nat. Rev. Mater. **6**, 201 (2021).

[2] Xiaomeng Liu, J. I. A. Li, Kenji Watanabe, Takashi Taniguchi, James Hone, Bertrand I. Halperin, Philip Kim, and Cory R. Dean, Crossover between strongly-coupled and weakly-coupled exciton superfluids, arXiv:2012.05916.

[3] Yuan Cao, Valla Fatemi, Shiang Fang, Kenji Watanabe, Takashi Taniguchi, Efthimios Kaxiras, and Pablo Jarillo-Herrero, Unconventional superconductivity in magic-angle graphene superlattices, Nature (London) **556**, 43 (2018).

[4] Rafi Bistritzer and Allan H. MacDonald, Moiré bands in twisted double-layer graphene, Proc. Natl. Acad. Sci. U.S.A. **108**, 12233 (2011).

[5] Emma C. Regan, Danqing Wang, Chenhao Jin, M. Iqbal Bakti Utama, Beini Gao, Xin Wei, Sihan Zhao, Wenyu

Zhao, Zuocheng Zhang, Kentaro Yumigeta, Mark Blei, Johan D. Carlström, Kenji Watanabe, Takashi Taniguchi, Sefaattin Tongay, Michael Crommie, Alex Zettl, and Feng Wang, Mott and generalized Wigner crystal states in WSe_2/WS_2 moiré superlattices, Nature (London) **579**, 359 (2020).

[6] Yanhao Tang, Lizhong Li, Tingxin Li, Yang Xu, Song Liu, Katayun Barmak, Kenji Watanabe, Takashi Taniguchi, Allan H. MacDonald, Jie Shan, and Kin Fai Mak, Simulation of Hubbard model physics in WSe_2/WS_2 moiré superlattices, Nature (London) **579**, 353 (2020).

[7] Yuya Shimazaki, Ido Schwartz, Kenji Watanabe, Takashi Taniguchi, Martin Kroner, and Ataç Imamoğlu, Strongly correlated electrons and hybrid excitons in a moiré heterostructure, Nature (London) **580**, 472 (2020).

[8] I. Ferrier-Barbut, M. Delehaye, S. Laurent, A. T. Grier, M. Pierce, B. S. Rem, F. Chevy, and C. Salomon, A mixture of Bose and Fermi superfluids, Science **345**, 1035 (2014).

[9] B. J. DeSalvo, Krutik Patel, Geyue Cai, and Cheng Chin, Observation of fermion-mediated interactions between bosonic atoms, Nature (London) **568**, 61 (2019).

[10] Isabella Fritsche, Cosetta Baroni, Erich Dobler, Emil Kirilov, Bo Huang, Rudolf Grimm, Georg M. Bruun, and Pietro Massignan, Stability and breakdown of Fermi polarons in a strongly interacting Fermi-Bose mixture, Phys. Rev. A **103**, 053314 (2021).

[11] Herman Feshbach, A unified theory of nuclear reactions. II, Ann. Phys. (N.Y.) **19**, 287 (1962).

[12] Cheng Chin, Rudolf Grimm, Paul Julienne, and Eite Tiesinga, Feshbach resonances in ultracold gases, Rev. Mod. Phys. **82**, 1225 (2010).

[13] Wolfgang Ketterle and Martin W. Zwierlein, Making, probing and understanding ultracold Fermi gases, Nuovo Cimento Riv. Ser. **31**, 247 (2008).

[14] Immanuel Bloch, Jean Dalibard, and Wilhelm Zwerger, Many-body physics with ultracold gases, Rev. Mod. Phys. **80**, 885 (2008).

[15] R. A. Duine and H. T. C. Stoof, Atom-molecule coherence in Bose gases, Phys. Rep. **396**, 115 (2004).

[16] Gang Wang, Alexey Chernikov, Mikhail M. Glazov, Tony F. Heinz, Xavier Marie, Thierry Amand, and Bernhard Urbaszek, Colloquium: Excitons in atomically thin transition metal dichalcogenides, Rev. Mod. Phys. **90**, 021001 (2018).

[17] E. V. Calman, L. H. Fowler-Gerace, D. J. Choksy, L. V. Butov, D. E. Nikonov, I. A. Young, S. Hu, A. Mishchenko, and A. K. Geim, Indirect excitons and trions in $MoSe_2/WSe_2$ van der Waals heterostructures, Nano Lett. **20**, 1869 (2020).

[18] Ido Schwartz, Yuya Shimazaki, Clemens Kuhlenkamp, Kenji Watanabe, Takashi Taniguchi, Martin Kroner, and Ataç Imamoğlu, Electrically tunable Feshbach resonances in twisted bilayer semiconductors, Science **374**, 336 (2021).

[19] The phenomenological treatment of the tunnel coupling t can break down for specific stackings: if the layer separation d is small, pronounced moire potentials with spatially modulated tunneling will form. In this case our phenomenological description is useful only for Fermi wavelengths much larger than the lattice constant of the superlattice.

[20] Large electric fields could overcome the energy difference resulting in sizable hybridization with interlayer excitons, which would then contribute to interlayer scattering of electrons and excitons. Here are we are interested in smaller fields on the order of the trion binding energy where these processes are suppressed.

[21] Christian Fey, Peter Schmelcher, Atac Imamoglu, and Richard Schmidt, Theory of exciton-electron scattering in atomically thin semiconductors, Phys. Rev. B **101**, 195417 (2020).

[22] J. J. Sakurai and Jim Napolitano, *Modern Quantum Mechanics*, 2nd ed. (Cambridge University Press, Cambridge, England, 2017).

[23] Steven Weinberg, *The Quantum Theory of Fields* (Cambridge University Press, Cambridge, England, 1995), Vol. 1.

[24] Sadhan K. Adhikari, Quantum scattering in two dimensions, Am. J. Phys. **54**, 362 (1986).

[25] Meera M. Parish and Jesper Levinsen, Highly polarized Fermi gases in two dimensions, Phys. Rev. A **87**, 033616 (2013).

[26] More importantly, for any given electron density, it is possible to choose E_z such that $k_F a_O \sim 1$, which yields the strong correlation regime.

[27] K. Kanjilal and D. Blume, Coupled-channel pseudopotential description of the Feshbach resonance in two dimensions, Phys. Rev. A **73**, 060701(R) (2006).

[28] See Supplemental Material at http://link.aps.org/supplemental/10.1103/PhysRevLett.129.037401 for a discussion of background scattering, our renormalization procedure, and details on the non-equilibrium T-matrix calculations, which includes Ref. [29].

[29] Mehrtash Babadi, *Non-Equilibrium Dynamics of Artificial Quantum Matter* (Harvard University, Cambridge, MA, 2013).

[30] Meinrad Sidler, Patrick Back, Ovidiu Cotlet, Ajit Srivastava, Thomas Fink, Martin Kroner, Eugene Demler, and Atac Imamoglu, Fermi polaron-polaritons in charge-tunable atomically thin semiconductors, Nat. Phys. **13**, 255 (2017).

[31] R. A. Suris, Correlation between trion and hole in Fermi distribution in process of trion photo-excitation in doped QWs, in *Optical Properties of 2D Systems with Interacting Electrons*, edited by Wolfgang J. Ossau and Robert Suris (Springer Netherlands, Dordrecht, 2003), pp. 111–124.

[32] Dmitry K. Efimkin and Allan H. MacDonald, Many-body theory of trion absorption features in two-dimensional semiconductors, Phys. Rev. B **95**, 035417 (2017).

[33] M. M. Glazov, Optical properties of charged excitons in two-dimensional semiconductors, J. Chem. Phys. **153**, 034703 (2020).

[34] N. Darkwah Oppong, L. Riegger, O. Bettermann, M. Höfer, J. Levinsen, M. M. Parish, I. Bloch, and S. Fölling, Observation of Coherent Multiorbital Polarons in a Two-Dimensional Fermi Gas, Phys. Rev. Lett. **122**, 193604 (2019).

[35] Finite momentum excitons are long-lived due to the steep light cone, which renders only $\mathbf{k} = 0$ excitons optically active.

[36] F. G. Fumi, Cxvi. Vacancies in monovalent metals, Lond. Edinb. Dublin Philos. Mag. J. Sci. **46**, 1007 (1955).

[37] Richard Schmidt, Michael Knap, Dmitri A. Ivanov, Jhih-Shih You, Marko Cetina, and Eugene Demler, Universal many-body response of heavy impurities coupled to a Fermi sea: A review of recent progress, Rep. Prog. Phys. **81**, 024401 (2018).
[38] F. Chevy, Universal phase diagram of a strongly interacting Fermi gas with unbalanced spin populations, Phys. Rev. A **74**, 063628 (2006).
[39] R. Combescot, A. Recati, C. Lobo, and F. Chevy, Normal State of Highly Polarized Fermi Gases: Simple Many-Body Approaches, Phys. Rev. Lett. **98**, 180402 (2007).
[40] Richard Schmidt, Tilman Enss, Ville Pietilä, and Eugene Demler, Fermi polarons in two dimensions, Phys. Rev. A **85**, 021602(R) (2012).
[41] Jonas Vlietinck, Jan Ryckebusch, and Kris Van Houcke, Diagrammatic Monte Carlo study of the Fermi polaron in two dimensions, Phys. Rev. B **89**, 085119 (2014).
[42] Peter Kroiss and Lode Pollet, Diagrammatic Monte Carlo study of quasi-two-dimensional Fermi polarons, Phys. Rev. B **90**, 104510 (2014).
[43] Marko Cetina, Michael Jag, Rianne S. Lous, Isabella Fritsche, Jook T. M. Walraven, Rudolf Grimm, Jesper Levinsen, Meera M. Parish, Richard Schmidt, Michael Knap, and Eugene Demler, Ultrafast many-body interferometry of impurities coupled to a Fermi sea, Science **354**, 96 (2016).
[44] Meera M. Parish, Polaron-molecule transitions in a two-dimensional Fermi gas, Phys. Rev. A **83**, 051603(R) (2011).
[45] Sascha Zöllner, G. M. Bruun, and C. J. Pethick, Polarons and molecules in a two-dimensional Fermi gas, Phys. Rev. A **83**, 021603(R) (2011).
[46] L. M. Sieberer, M. Buchhold, and S. Diehl, Keldysh field theory for driven open quantum systems, Rep. Prog. Phys. **79**, 096001 (2016).
[47] Tomasz Wasak, Richard Schmidt, and Francesco Piazza, Quantum-zeno Fermi polaron in the strong dissipation limit, Phys. Rev. Research **3**, 013086 (2021).
[48] C. Kohstall, M. Zaccanti, M. Jag, A. Trenkwalder, P. Massignan, G. M. Bruun, F. Schreck, and R. Grimm, Metastability and coherence of repulsive polarons in a strongly interacting Fermi mixture, Nature (London) **485**, 615 (2012).
[49] H. H. Fang, B. Han, C. Robert, M. A. Semina, D. Lagarde, E. Courtade, T. Taniguchi, K. Watanabe, T. Amand, B. Urbaszek, M. M. Glazov, and X. Marie, Control of the Exciton Radiative Lifetime in van der Waals Heterostructures, Phys. Rev. Lett. **123**, 067401 (2019).
[50] Jason S. Ross, Sanfeng Wu, Hongyi Yu, Nirmal J. Ghimire, Aaron M. Jones, Grant Aivazian, Jiaqiang Yan, David G. Mandrus, Di Xiao, Wang Yao, and Xiaodong Xu, Electrical control of neutral and charged excitons in a monolayer semiconductor, Nat. Commun. **4**, 1474 (2013).
[51] P. Massignan, Polarons and dressed molecules near narrow Feshbach resonances, Europhys. Lett. **98**, 10012 (2012).
[52] N. Takemura, S. Trebaol, M. Wouters, M. T. Portella-Oberli, and B. Deveaud, Polaritonic Feshbach resonance, Nat. Phys. **10**, 500 (2014).
[53] Fabrice P. Laussy, Alexey V. Kavokin, and Ivan A. Shelykh, Exciton-Polariton Mediated Superconductivity, Phys. Rev. Lett. **104**, 106402 (2010).
[54] Ovidiu Cotleţ, Sina Zeytinoğlu, Manfred Sigrist, Eugene Demler, and Ataç Imamoğlu, Superconductivity and other collective phenomena in a hybrid Bose-Fermi mixture formed by a polariton condensate and an electron system in two dimensions, Phys. Rev. B **93**, 054510 (2016).
[55] Zefang Wang, Daniel A. Rhodes, Kenji Watanabe, Takashi Taniguchi, James C. Hone, Jie Shan, and Kin Fai Mak, Evidence of high-temperature exciton condensation in two-dimensional atomic double layers, Nature (London) **574**, 76 (2019).
[56] Long Zhang, Zhe Zhang, Fengcheng Wu, Danqing Wang, Rahul Gogna, Shaocong Hou, Kenji Watanabe, Takashi Taniguchi, Krishnamurthy Kulkarni, Thomas Kuo, Stephen R. Forrest, and Hui Deng, Twist-angle dependence of moiré excitons in $WS_2/MoSe_2$ heterobilayers, Nat. Commun. **11**, 5888 (2020).
[57] V. Efimov, Energy levels arising from resonant two-body forces in a three-body system, Phys. Lett. **33B**, 563 (1970).
[58] V. N. Efimov, Weakly bound states of three resonantly interacting particles, Yad. Fiz. **12**, 1080 (1970).
[59] Kevin Slagle and Liang Fu, Charge transfer excitations, pair density waves, and superconductivity in moiré materials, Phys. Rev. B **102**, 235423 (2020).